SEMARAK ILMU PUBLISHING

Semarak Engineering Journal

Journal homepage:
https://semarakilmu.my/index.php/sej/index
ISSN: 3036-0145



Improving the Efficiency of Horizontal-Axis Wind Turbines Using High-Lift Devices

Qassim Wanis M.[1,*], Muhammad A. R. Yass[1], Ahmed Kamil Hasan[1]

[1] Department of Electromechanical Engineering, University of Technology, Iraq

ARTICLE INFO

Article history:
Received 13 May 2026
Received in revised form 20 August 2026
Accepted 22 September 2026
Available online 30 October 2026

Keywords:
Wind turbine efficiency; High lift devices; Flap; Aerodynamic Enhancement; Aerodynamic control

ABSTRACT

This study investigates the potential of trailing-edge flaps to enhance the aerodynamic performance, efficiency, and energy capture of horizontal-axis wind turbines. Three airfoil profiles, FX66-S-196V, FX63-137 S, and SG6043, were incorporated at different radial positions along the turbine blades. Trailing-edge flaps were introduced as active aerodynamic control devices to regulate aerodynamic forces and improve blade performance under varying wind conditions. Computational fluid dynamics (CFD) simulations and optimization techniques were employed to evaluate the effects of flap deployment on turbine aerodynamic characteristics. The influences of flap deflection angle, position, and deployment strategy were examined in terms of power coefficient, lift-to-drag ratio, and energy extraction efficiency. The results indicate that appropriate flap deployment can improve turbine performance, with predicted power output enhancements ranging from 2.5% to 4.6%, depending on operating conditions, including wind speed, tip-speed ratio, angle of attack, and flap deflection angle. Furthermore, sensitivity analysis identified favorable flap configurations under different wind regimes, emphasizing the potential benefits of adaptive aerodynamic control strategies. These findings demonstrate the potential of trailing-edge flaps to improve wind turbine aerodynamic efficiency and energy capture, providing a basis for further development and experimental validation of active aerodynamic control systems for horizontal-axis wind turbines.

1. Introduction

Wind energy has become an increasingly important source of renewable electricity, contributing to global efforts to reduce dependence on conventional energy resources and promote sustainable power generation. The aerodynamic performance of wind turbine blades plays a fundamental role in determining the efficiency of wind energy conversion systems, as the blades are responsible for extracting kinetic energy from the wind and converting it into mechanical rotational energy.

* *Corresponding author.*
E-mail address: eme.22.22@grad.uotechnology.edu.iq

https://doi.org/10.37934/sej.16.1.250265

Improving blade aerodynamic efficiency is therefore essential for enhancing turbine performance, increasing power generation, and reducing the cost of wind energy production [7–9].

Conventional horizontal-axis wind turbine (HAWT) blades are designed using airfoil profiles selected to achieve favorable aerodynamic performance under specified operating conditions. However, variations in wind speed, angle of attack, and local flow conditions along the blade span can influence aerodynamic loading and energy extraction efficiency. Consequently, advancements in aerodynamic design have encouraged the development of optimized blade geometries, multiple-airfoil configurations, and aerodynamic control devices to improve turbine performance under varying operating conditions [1, 2, 5, 10].

One promising approach involves incorporating multiple airfoil sections along the blade radius, with each section selected according to its aerodynamic characteristics and local operating requirements. This configuration allows the blade geometry to accommodate variations in relative wind velocity, Reynolds number, and aerodynamic loading along the span. Furthermore, the integration of high-lift devices, particularly trailing-edge flaps, provides an additional means of modifying the aerodynamic forces acting on the blade. By adjusting the flap deflection angle, the effective airfoil camber and aerodynamic loading can be altered, potentially improving the lift-to-drag ratio and power extraction under selected operating conditions [11–13].

Several researchers have investigated the effects of airfoil selection, blade geometry optimization, and aerodynamic modifications on HAWT performance. Muheisen *et al*., [1] investigated the aerodynamic performance of multi-section HAWT blades with and without aerodynamic fences. Different airfoil sections were distributed along the blade radius, and a NACA 4412 blade of identical dimensions was employed as a reference configuration. Their results indicated that the multi-section blade configuration improved the power coefficient by approximately 8%, corresponding to an additional 40 W for a small wind turbine with a diameter of 127 cm and a rated output of 500 W. The incorporation of aerodynamic fences at experimentally determined positions further improved the reported power coefficient by approximately 16%, while maintaining favorable flutter stability.

Hussein *et al*., [2] employed computational fluid dynamics (CFD) simulations and blade optimization approaches based on the Schmitz and Betz methods to investigate the effects of chord length, twist angle, and airfoil selection on wind turbine performance. Symmetrical, asymmetrical, and supercritical airfoil profiles were considered to evaluate their aerodynamic characteristics. The combination of Schmitz-based chord optimization and lift-to-drag-ratio-based twist adjustment produced improvements in the power coefficient of approximately 10.3%, 9.5%, and 16% for the Eppler 417, NACA 4412, and NACA 0012 airfoils, respectively. These findings demonstrated the importance of blade geometry and airfoil selection in improving wind energy extraction.

Rasheed *et al*., [3] investigated the influence of the lift-to-drag ratio (C_l/C_D) on the power coefficient of HAWT blades incorporating different airfoil cross-sections. Their study considered symmetrical, asymmetrical, and supercritical airfoil configurations to determine suitable lift-to-drag-ratio distributions and corresponding angles of attack along the blade span. The reported maximum power coefficients were approximately 0.47, 0.49, and 0.48 for the NACA 4412, Eppler, and NACA 0012 airfoils, respectively. The findings highlighted the importance of optimizing the lift-to-drag ratio and angle-of-attack distribution to improve overall turbine performance.

Yass *et al*., [4] conducted an experimental and numerical investigation of a HAWT blade incorporating the symmetrical NACA 0012 airfoil. The blade was designed, analyzed, optimized, and manufactured to evaluate the effects of geometric modifications on turbine performance. A computational program developed using Fortran 90 was employed to calculate the blade design parameters, and the results were compared with CFD predictions. The Schmitz, Betz, and lift-to-drag-

ratio optimization methods were applied to improve the chord and twist distributions. At a tip-speed ratio (TSR) of 7, the initial power coefficient was approximately 0.481. Following optimization, the maximum power coefficient increased to 0.556 using Schmitz chord modification combined with lift-to-drag-ratio-based twist optimization. The corresponding power coefficient obtained using Betz chord modification and lift-to-drag-ratio-based twist optimization was approximately 0.53.

Xi and Zhao [5] investigated the aerodynamic optimization of wind turbine blades using combinations of multiple NACA airfoil profiles. The airfoils were selected and distributed along the blade span according to their geometric characteristics, including thickness and camber, to develop a blade configuration incorporating multiple airfoil sections. The aerodynamic performance of the resulting blade was evaluated using computational methods. Their findings indicated that combining different airfoil profiles could improve the wind energy utilization coefficient, demonstrating the potential of multi-airfoil configurations for enhancing wind turbine efficiency.

Akbari *et al*., [6] performed a multi-objective optimization study on a small HAWT blade to improve its starting characteristics under low wind-speed conditions. The blade was divided into two radial regions, with the boundary located at approximately r/R = 0.52. The chord length and twist angle were modified to improve the starting torque while maintaining acceptable aerodynamic performance. The optimized configuration reportedly reduced the power coefficient by approximately 1.5% but enabled turbine operation at a wind speed of 4 m/s instead of 6 m/s. These findings demonstrated the potential trade-off between maximum aerodynamic efficiency and improved low-wind-speed starting performance.

Previous investigations have demonstrated that airfoil selection, blade geometry optimization, and aerodynamic modifications can substantially influence HAWT performance [1–6]. Nevertheless, further investigation is warranted to evaluate the combined influence of multiple airfoil sections and trailing-edge flap deployment on aerodynamic performance under different operating conditions. In particular, the effects of flap deflection angle, flap position, and operating parameters on the power coefficient and lift-to-drag ratio require systematic evaluation.

Therefore, the present study investigates the aerodynamic performance of a horizontal-axis wind turbine incorporating multiple airfoil sections and trailing-edge flaps. The FX66-S-196V, FX63-137 S, and SG6043 airfoil profiles are distributed along the blade radius to establish a multi-section blade configuration. CFD simulations are employed to evaluate the influence of flap deployment and operating conditions, including wind speed, tip-speed ratio, angle of attack, and flap deflection angle, on the aerodynamic performance of the turbine. The study aims to identify favorable flap configurations, assess their effects on power extraction, and provide insights into the potential application of trailing-edge flaps as aerodynamic control devices for improving HAWT efficiency.

2. Theoretical Analysis

The fundamental principles governing the design and operation of wind turbines are based on the aerodynamic interaction between the wind and the turbine rotor. These principles apply to both horizontal-axis and vertical-axis wind turbines. The aerodynamic efficiency of a wind turbine is commonly expressed in terms of the power coefficient (Cp), which represents the ratio of the mechanical power extracted by the rotor to the total kinetic power available in the incoming wind. According to Betz's theory, the maximum theoretical power coefficient of an ideal wind turbine is 0.593, corresponding to approximately 59.3% of the available wind power [7].

The power coefficient is expressed as:

$$C_p = \frac{P_{\text{rotor}}}{\frac{1}{2}\rho A V^3}$$

where P_{rotor} is the mechanical power extracted by the rotor, ρ is the air density (kg/m³), A is the rotor swept area (m²), and V is the undisturbed wind velocity (m/s).

2.1 Lift and Drag Forces

Lift and drag are the primary aerodynamic forces acting on wind turbine blades. Their magnitudes depend on the lift coefficient C_L, drag coefficient C_D, airfoil geometry, and angle of attack α. The aerodynamic coefficients vary with the blade cross-sectional profile and the flow conditions experienced by the blade [10].

The lift force is calculated using:

$$L = \frac{1}{2}\rho V_a^2 A C_L$$

The drag force is expressed as:

$$D = \frac{1}{2}\rho V_a^2 A C_D$$

The drag force acts parallel to the relative airflow direction, whereas the lift force acts perpendicular to it [11]. For wind turbine blades, the combined effects of lift and drag determine the aerodynamic forces contributing to rotor torque and power generation. Therefore, maximizing the lift-to-drag ratio is an important consideration in improving wind turbine aerodynamic performance.

3. Flaps

Flaps are aerodynamic control devices used to modify the lift characteristics of an airfoil by altering its effective camber and pressure distribution. Increasing the lift generated by an airfoil generally requires an increase in circulation while maintaining sufficiently attached airflow. Trailing-edge flaps achieve this primarily by modifying the camber near the trailing edge, thereby changing the aerodynamic loading and increasing the lift coefficient under suitable operating conditions [12].

When a trailing-edge flap is deflected downward, the effective camber of the airfoil increases, producing a corresponding change in circulation and shifting the zero-lift angle of attack α_{0L} toward more negative values. This shift allows the airfoil to generate a higher lift coefficient at a given geometric angle of attack. In comparison, changes in camber near the leading edge generally have a smaller influence on the zero-lift angle of attack.

The zero-lift angle of attack, α_{0L}, is defined as the angle between the reference chord line of the unflapped airfoil and the freestream velocity at which the lift coefficient becomes zero.

Although trailing-edge flaps can increase lift, they do not necessarily delay flow separation. Increasing flap deflection may intensify adverse pressure gradients and promote boundary-layer separation, particularly at higher angles of attack. Consequently, excessive flap deflection can increase aerodynamic drag and reduce the lift-to-drag ratio. The effectiveness of trailing-edge flaps also depends on blade geometry, including sweep angle, flap dimensions, and operating conditions. In particular, trailing-edge flaps generally become less effective as blade sweep increases [12].

Therefore, the selection of an appropriate flap configuration and deflection angle is essential for achieving favorable aerodynamic performance without introducing excessive drag or flow separation.

3.1 Calculation of the Maximum Lift Coefficient with Flap Deployment

The increase in the maximum lift coefficient resulting from trailing-edge flap deployment can be estimated by considering the maximum lift increment of the flapped airfoil section, the proportion of blade area equipped with flaps, and a correction factor accounting for finite-blade effects [12].

The increase in the maximum lift coefficient is expressed as:

$$\Delta C_{L,\max} = (\Delta C_{L,\max})_{\text{section}} \left(\frac{S_{Wf}}{S_W} \right) K$$

where:

- $\Delta C_{L,\max}$ is the estimated increase in the maximum lift coefficient of the blade;
- $(\Delta C_{L,\max})_{\text{section}}$ is the increase in the maximum lift coefficient of the flapped airfoil section, which can be determined experimentally or from suitable aerodynamic data;
- S_{Wf} is the blade area associated with the flapped region (m²);
- S_W is the total reference blade area (m²); and
- K is an empirical correction factor accounting for finite-blade and geometric effects.

The maximum lift coefficient of the flapped blade can then be estimated by adding the calculated lift increment to the maximum lift coefficient of the unflapped blade:

$$C_{L,\max,\text{flapped}} = C_{L,\max,\text{unflapped}} + \Delta C_{L,\max}$$

The corresponding lift curve can be constructed by incorporating the estimated increase in maximum lift coefficient and the change in zero-lift angle of attack resulting from flap deployment. Figure 1 illustrates the construction of blade lift curves for a mechanical high-lift device.

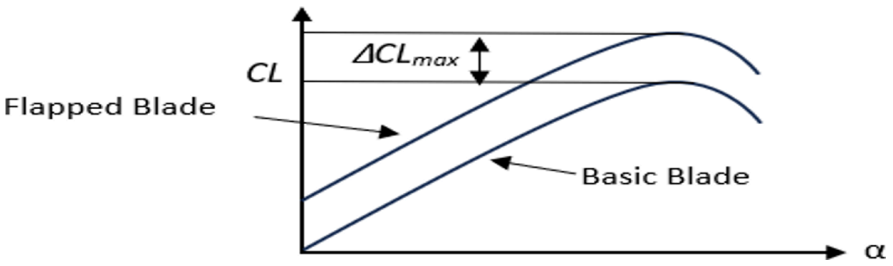


Fig. 1. Construction of Blade Lift Curves for a Mechanical High-Lift Device

The change in zero-lift angle of attack $\nabla\alpha_{0L}$ can be estimated from the aerodynamic characteristics of the flapped airfoil section. However, the resulting lift enhancement depends on the flap geometry, deflection angle, and blade configuration. In particular, the effectiveness of trailing-edge flaps may decrease for highly swept blades because of three-dimensional aerodynamic effects [12].

Equation above provides an approximate method for estimating the influence of flap deployment on the maximum lift coefficient. For rotating wind turbine blades, additional aerodynamic effects associated with radial flow, rotational augmentation, and three-dimensional blade geometry may influence the actual lift characteristics. Therefore, computational fluid dynamics simulations are

employed in the present study to evaluate the aerodynamic performance of the proposed flap configurations under the investigated operating conditions.

4. Experimental Work

The rotor is a fundamental component of a wind turbine, responsible for converting the kinetic energy of the wind into mechanical rotational energy. Its aerodynamic performance directly influences the generated torque, rotational speed, and overall power output. In the present study, a horizontal-axis wind turbine (HAWT) equipped with three blades was designed and fabricated. As illustrated in Figure 2, each blade had a span of 0.56 m and a base chord length of 0.10 m. The specifications of the developed HAWT are presented in Table 1, while the three-bladed wind turbine incorporating multiple airfoil cross-sections is shown in Figure 3.

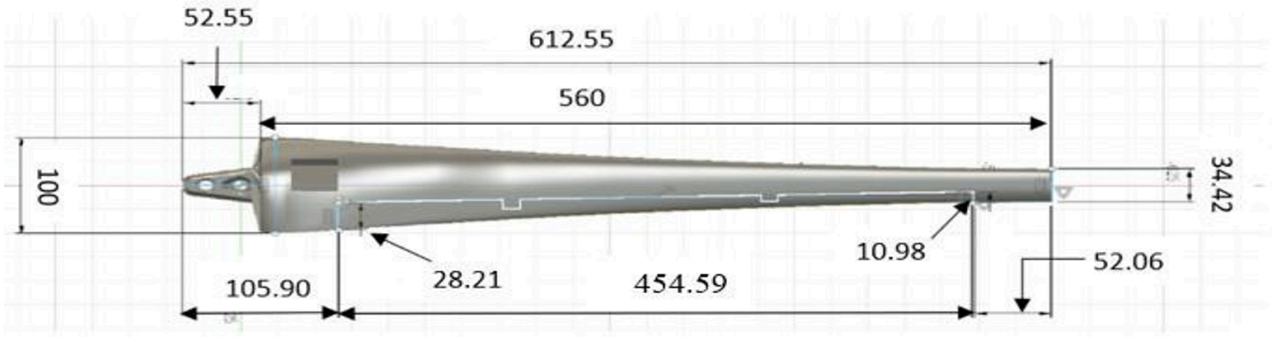


Fig. 2. Geometric Dimensions of the Multi-Section Wind Turbine Blade Equipped with Trailing-Edge Flaps (All Dimensions in mm)



Fig. 3. Three-Dimensionally Printed Multi-Section Wind Turbine Blades Equipped with Trailing-Edge Flaps

Table 1
Geometric Specifications of the Horizontal-Axis Wind Turbine

Parameter	Specification
Rotor diameter	1.251 m
Hub diameter	0.130 m
Blade span	0.560 m
Base chord length	0.100 m

The aerodynamic and geometric parameters of the blades were selected to enhance wind energy extraction and improve the power coefficient. During the design and optimization process, each rotor blade was divided into multiple sections, allowing its geometric characteristics to vary along the blade span. Each section was defined by its radial position, chord length, twist angle, and airfoil profile. The three-dimensional blade geometry was developed using Autodesk Fusion 360, considering the aerodynamic characteristics and estimated inflow angle at each blade section. A computational program was employed to determine the geometric parameters required for blade design.

The three-dimensional blade models were subsequently fabricated using a 3D printer with polylactic acid (PLA) as the printing material. Each fabricated blade had a mass of approximately 200 g. Figure 4 illustrates the multi-section wind turbine blade equipped with trailing-edge flaps. The flaps were installed at experimentally determined positions along the blade to investigate their influence on aerodynamic performance. A programmable digital servo motor was employed to regulate the flap deflection angle, enabling adjustments to the blade's aerodynamic characteristics under different operating conditions [13].

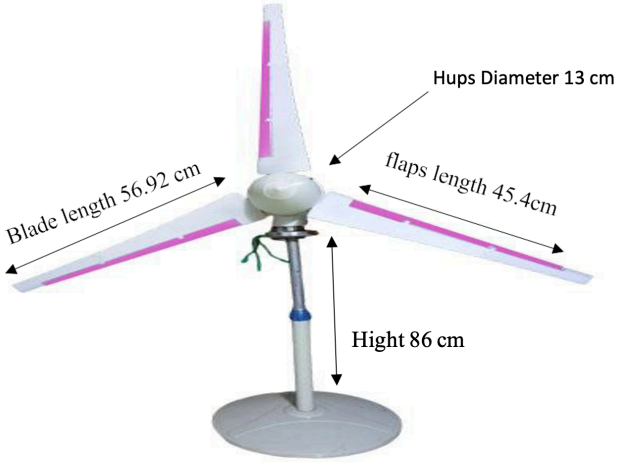


Fig. 4. Experimental Setup of the Three-Bladed Horizontal-Axis Wind Turbine Equipped with Trailing-Edge Flaps, Showing the Main Geometric Dimensions

4. Results and Discussion

The aerodynamic performance of the multi-section horizontal-axis wind turbine (HAWT) was evaluated to investigate the effects of trailing-edge flap deployment on lift coefficient, drag coefficient, lift-to-drag ratio, and power coefficient. The results indicate that incorporating trailing-edge flaps modifies the aerodynamic characteristics of the turbine blades, with the magnitude of the changes depending on the operating conditions and flap deflection angle. In particular, flap deployment increased the reported lift coefficient, although it also increased the drag coefficient. Consequently, the overall aerodynamic benefit depends on the balance between lift enhancement and the associated drag penalty.

4.1 Effect of tip-speed ratio on lift coefficient

Figure 5 and Table 2 illustrate the variation in lift coefficient C_L with tip-speed ratio λ for blade configurations with and without flaps. The lift coefficient increased with tip-speed ratio up to $\lambda = 2.5$,

after which a slight reduction was observed. At $\lambda = 2.5$, the lift coefficient increased from 2.34 without flaps to approximately 2.873 with flaps, corresponding to an absolute increase of approximately 0.533, or 22.8%. This result indicates that trailing-edge flap deployment increased the calculated lift coefficient throughout the investigated tip-speed-ratio range.

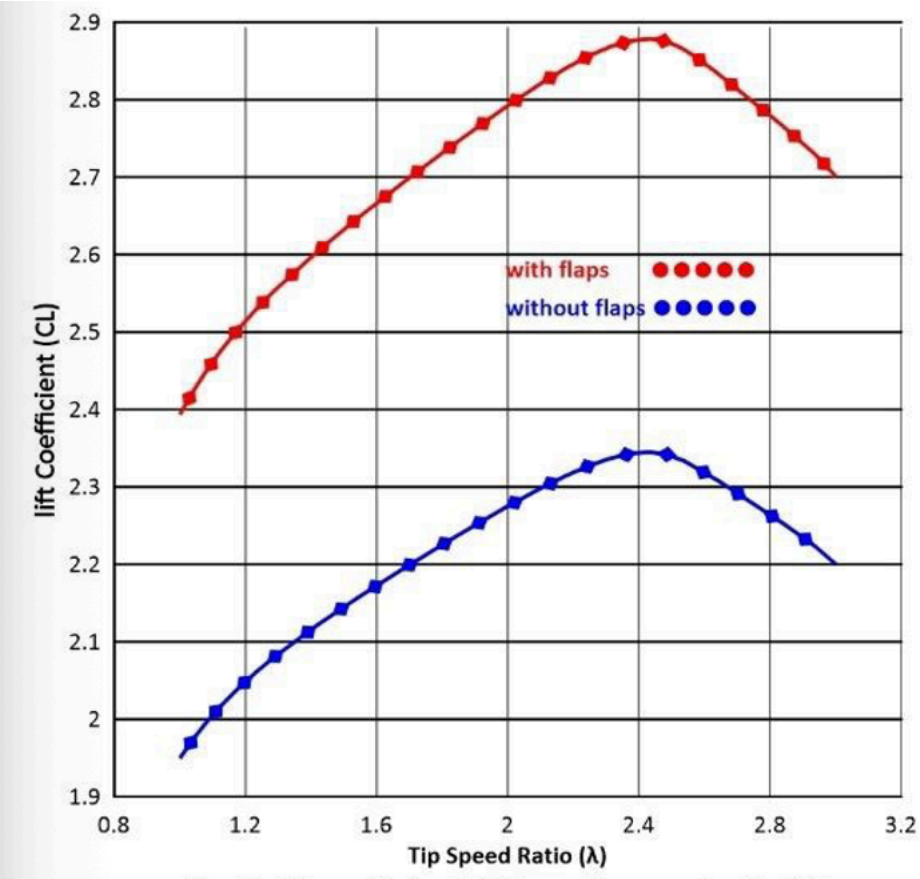


Fig. 5. Variation in Lift Coefficient C_L with Tip-Speed Ratio λ for Wind Turbine Blades With and Without Trailing-Edge Flaps

Table 2
Variation in Lift Coefficient with Tip-Speed Ratio for Wind Turbine Blades With and Without Flaps

Tip-speed ratio, λ	C_L without flaps	C_L with flaps
1.0	1.95	2.393865
1.5	2.12	2.602560
2.0	2.32	2.848085
2.5	2.34	2.872637
3.0	2.20	2.700770

4.2 Effect of angle of attack on lift coefficient

The relationship between lift coefficient and angle of attack α at a flap deflection angle of 5° is presented in Figure 6 and Table 3. The lift coefficient increased progressively with angle of attack, reaching its maximum reported value at 19.5°. At this angle, the lift coefficient increased from 2.34 without flaps to approximately 2.873 with flaps. A slight decrease was observed at 21°, suggesting

that further increases in angle of attack did not produce additional lift enhancement under the investigated conditions. However, this trend alone is insufficient to establish the onset of stall without additional aerodynamic evidence.

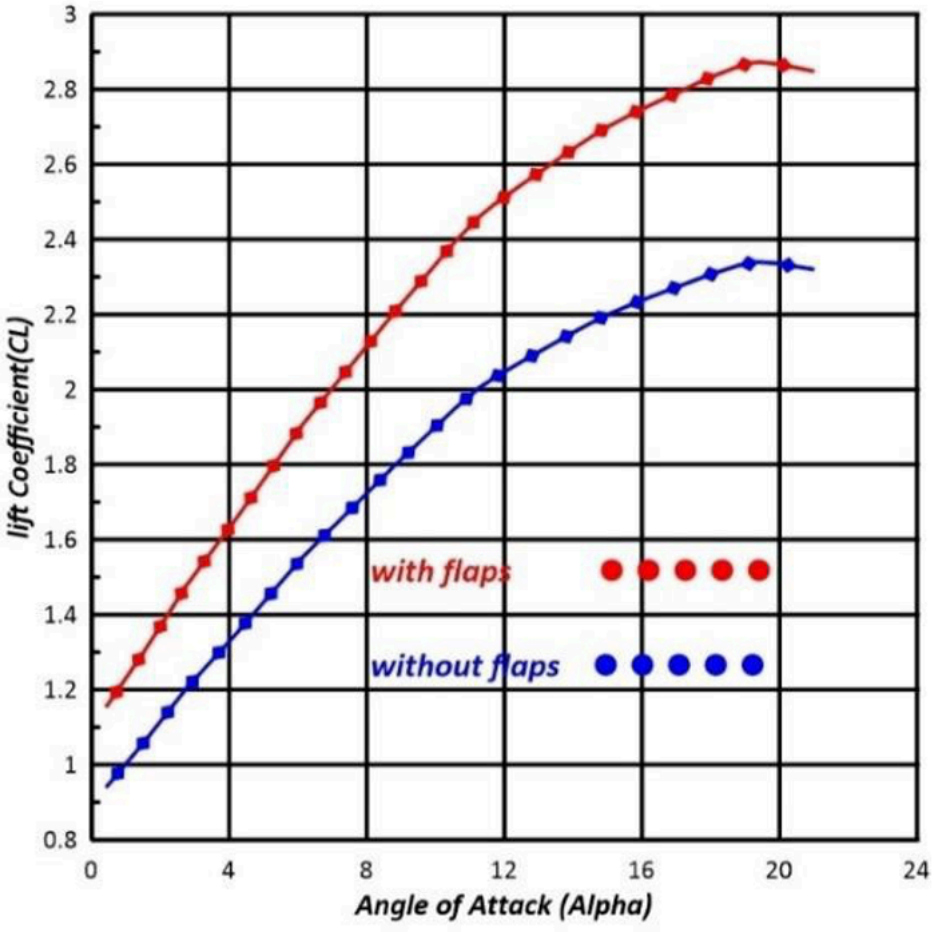


Fig. 6. Variation in Lift Coefficient C_L with Angle of Attack α for Wind Turbine Blades With and Without Trailing-Edge Flaps at a Flap Deflection Angle of 5°

Table 3
Variation in Lift Coefficient with Angle of Attack for Wind Turbine Blades With and Without Flaps at a Flap Deflection Angle of 5°

Angle of attack, α°	C_L without flaps	C_L with flaps
0.42	0.94	1.153965
1.52	1.06	1.301280
2.72	1.20	1.473147
4.21	1.35	1.657291
6.10	1.55	1.902815
8.50	1.77	2.172892
11.20	2.00	2.455246
15.00	2.20	2.700770
19.50	2.34	2.872637
21.00	2.32	2.848085

4.3 Effect of rotational speed on drag coefficient

Figure 7 and Table 4 present the variation in drag coefficient ((C_D)) with turbine rotational speed. The results indicate that the drag coefficient generally decreased as rotational speed increased, although a slight increase was observed at the highest investigated rotational speed. The drag coefficient was consistently higher for the configuration with flaps than for the configuration without flaps. For example, at 228.846 rpm, the drag coefficient increased from 0.321620 to 0.394828 following flap deployment. This increase demonstrates that the additional lift generated by the trailing-edge flaps was accompanied by an aerodynamic drag penalty.

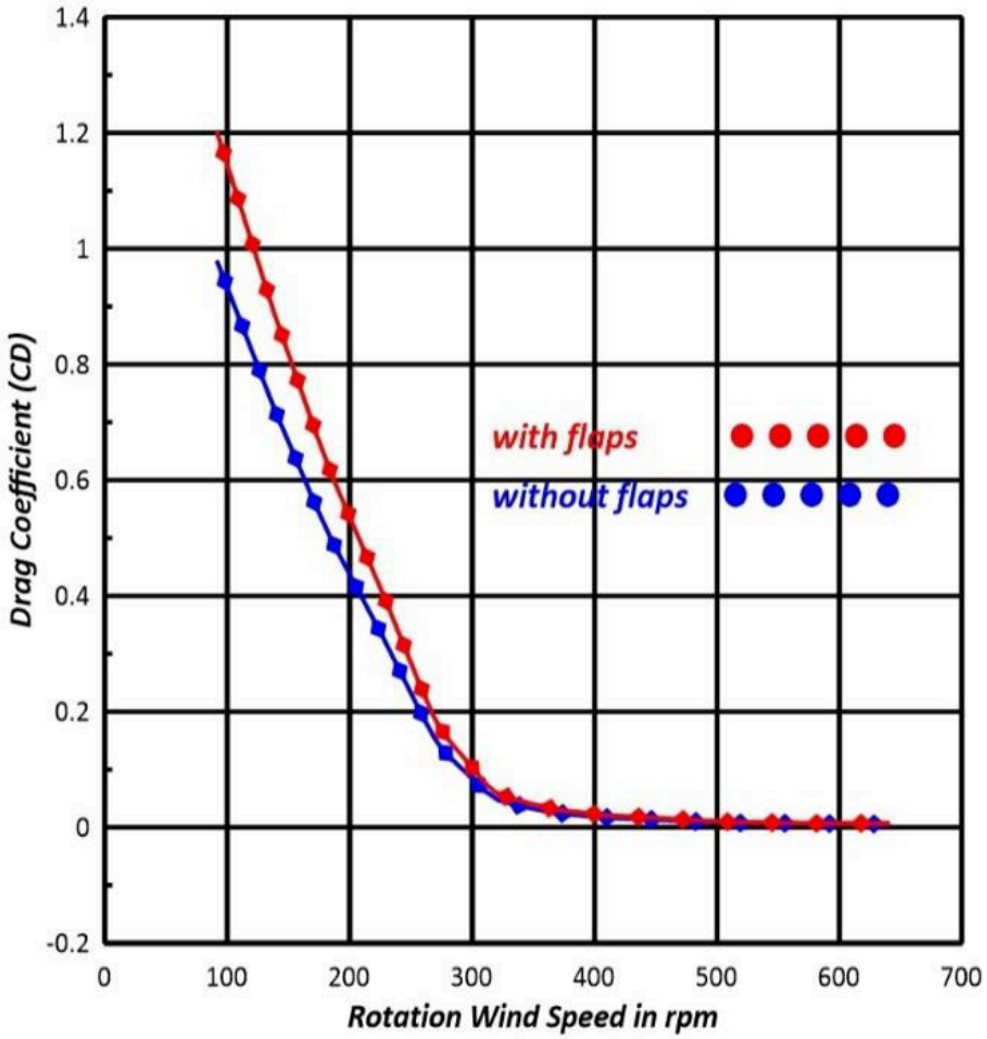


Fig. 7. Variation in Drag Coefficient C_D with Turbine Rotational Speed (rpm) for Wind Turbine Blades With and Without Trailing-Edge Flaps

Table 4
Variation in Drag Coefficient with Turbine Rotational Speed for Blade Configurations With and Without Flaps

Rotational speed (rpm)	C_D without flaps	C_D with flaps
91.5385	0.978778	1.201570
137.308	0.729070	0.895023
183.077	0.505359	0.620390
228.846	0.321620	0.394828
274.616	0.137753	0.169109
320.385	0.0481927	0.059162
366.154	0.0256785	0.031524
411.923	0.0166524	0.020443
457.693	0.0116757	0.014333
503.462	0.00806251	0.009898
549.231	0.00632352	0.007763
595.000	0.0056094	0.006886
640.770	0.00592765	0.007277

4.4 Effect of rotational speed on lift-to-drag ratio

The variation in lift-to-drag ratio C_L/C_D with rotational speed is presented in Figure 8 and Table 5. The results show that the lift-to-drag ratio was higher for the flapped configuration at every reported rotational speed. At 595 rpm, the ratio increased from approximately 188.969 without flaps to 199.665 with flaps. These findings suggest that, despite the increase in drag coefficient, the reported lift enhancement resulted in a modest improvement in the lift-to-drag ratio. Nevertheless, the magnitude of the calculated ratios and their consistency with the lift and drag coefficient data require verification before definitive aerodynamic conclusions can be drawn.

Table 5
Variation in Lift-to-Drag Ratio with Turbine Rotational Speed for Blade Configurations With and Without Flaps

Rotational speed (rpm)	C_L/C_D without flaps	C_L/C_D with flaps
91.5385	1.9922	2.0535
137.308	2.90781	2.9901
183.077	4.5907	4.7095
228.846	7.24457	7.4311
274.616	16.9869	17.4224
320.385	45.6500	46.8950
366.154	77.1073	79.4438
411.923	106.891	110.4945
457.693	132.754	137.8932
503.462	168.681	176.1238
549.231	189.767	199.2561
595.000	188.9685	199.6648
640.770	160.265	170.3879

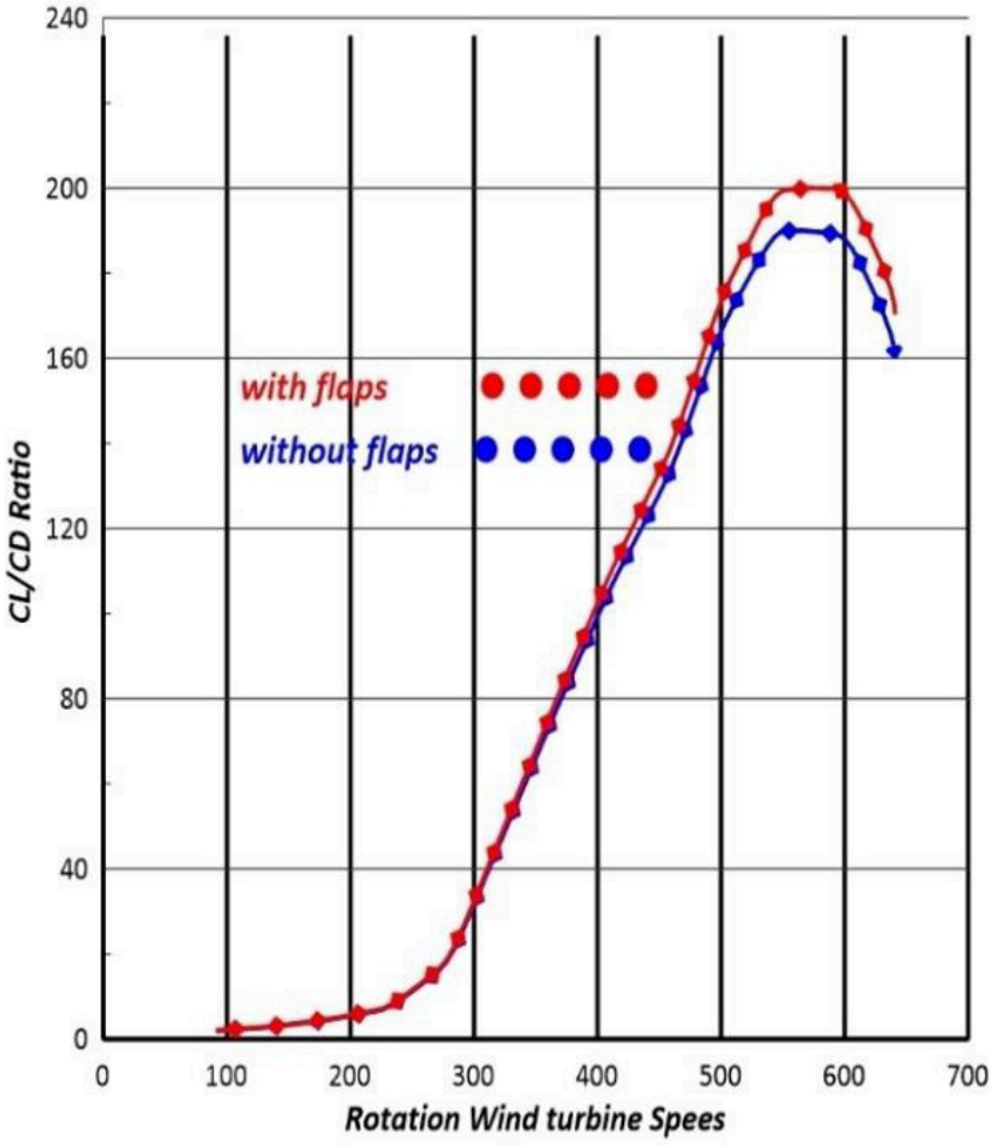


Fig. 8. Variation in Lift-to-Drag Ratio C_L/C_D with Turbine Rotational Speed (rpm) for Wind Turbine Blades With and Without Trailing-Edge Flaps

4.5 Effect of flap deflection angle on power coefficient

Tables 6–8 compare the reported power coefficients C_p for configurations with and without trailing-edge flaps at flap deflection angles of 20°, 10°, and 5°, respectively. The results indicate that flap deployment generally increased the reported power coefficient over the investigated operating conditions, although some reductions occurred at lower rotational speeds for the 5° configuration. The largest absolute differences between the paired power coefficients were approximately 0.0993 at 20°, 0.0846 at 10°, and 0.0553 at 5°. However, the rotational speeds of the flapped and unflapped configurations differed within each comparison. Therefore, these differences should be interpreted

as comparisons between the reported operating points rather than as isolated effects of flap deployment at identical rotational speeds.

Table 6
Comparison of Power Coefficients for Wind Turbine Configurations With and Without Flaps at a Flap Deflection Angle of 20° and a Wind Speed of 3 m/s

Speed without flaps (rpm)	C_p without flaps	Speed with flaps (rpm)	C_p with flaps	Reported ∇C_p
45.7693	0.041005	68.7693	0.073424966	0.03242037
68.6539	0.073135	91.6539	0.131035410	0.05790011
91.5385	0.130578	114.5385	0.221784393	0.09120639
114.423	0.221285	137.423	0.320571356	0.09928636
137.308	0.320234	160.308	0.387593883	0.06735988
160.192	0.387365	183.192	0.432681864	0.04531686
183.077	0.432520	206.077	0.464840181	0.03232018
205.962	0.464731	228.962	0.486515114	0.02178411
228.846	0.486457	251.846	0.497937704	0.01148070
251.731	0.497922	274.731	0.500959443	0.00303744

Table 7
Comparison of Power Coefficients for Wind Turbine Configurations With and Without Flaps at a Flap Deflection Angle of 10° and a Wind Speed of 3 m/s

Speed without flaps (rpm)	C_p without flaps	Speed with flaps (rpm)	C_p with flaps	Reported ∇C_p
45.7693	0.041005	63.7693	0.060874452	0.01986985
68.6539	0.073135	86.6539	0.111216973	0.03808167
91.5385	0.130578	109.5385	0.200165647	0.06958765
114.423	0.221285	132.423	0.305903685	0.08461868
137.308	0.320234	155.308	0.377728250	0.05749425
160.192	0.387365	178.192	0.425644285	0.03827929
183.077	0.432520	201.077	0.460093196	0.02757320
205.962	0.464731	223.962	0.484010198	0.01927920
228.846	0.486457	246.846	0.497254942	0.01079794
251.731	0.497922	269.731	0.504766252	0.00684425

Table 8
Comparison of Power Coefficients for Wind Turbine Configurations With and Without Flaps at a Flap Deflection Angle of 5° and a Wind Speed of 3 m/s

Speed without flaps (rpm)	C_p without flaps	Speed with flaps (rpm)	C_p with flaps	Calculated ∇C_p
45.7693	0.041005	53.7693	0.035773423	−0.00523158
68.6539	0.073135	76.6539	0.071580101	−0.00155490
91.5385	0.130578	99.5385	0.156928155	0.02635016
114.423	0.221285	122.423	0.276568341	0.05528334
137.308	0.320234	145.308	0.357996985	0.03776299
160.192	0.387365	168.192	0.411569127	0.02420413
183.077	0.432520	191.077	0.450599226	0.01807923

Table 9 summarizes the reported performance improvements for the three flap deflection angles. The highest reported improvement was 4.6% at a flap angle of 20° and a rotational speed of 343 rpm, followed by 3.7% at 10° and 338 rpm and 2.5% at 5° and 328 rpm. These results suggest that increasing flap deflection may improve the reported power coefficient within the investigated range. However, because the operating speeds also differed, the results do not independently establish flap angle as the sole cause of the observed improvements.

Table 9
Summary of Reported Power Coefficient Improvements at Different Flap Deflection Angles

Flap angle (°)	Area under C_p curve	Rotational speed (rpm)	Reported improvement
5	73.69776731	328	2.5%
10	77.74427914	338	3.7%
20	79.65311004	343	4.6%

4.6 Low-wind-speed operation and comparison with previous studies

An additional objective of incorporating trailing-edge flaps was to improve turbine operation under low wind-speed conditions. The study reports that the turbine without flaps began rotating at a wind speed of approximately 3 m/s, whereas the configuration with flaps began rotating at approximately 1.4 m/s. This observation suggests that flap deployment may improve the starting characteristics of the investigated turbine. However, repeated start-up measurements and corresponding torque data are required to establish the reproducibility of this result.

Previous investigations have examined aerodynamic modifications, blade optimization, and performance enhancement for wind and related turbine configurations [14–19]. The present study focuses specifically on the application of trailing-edge flaps to a multi-section HAWT intended for low-wind-speed operation. Nevertheless, differences in turbine geometry, operating conditions, and evaluation methods limit direct quantitative comparisons with these studies.

Overall, the reported results indicate that trailing-edge flap deployment can increase the lift coefficient and modestly improve the lift-to-drag ratio and reported power coefficient of the investigated turbine. These benefits are accompanied by increased aerodynamic drag.

5. Conclusion

This study investigated the effects of trailing-edge flaps on the aerodynamic performance of a multi-section horizontal-axis wind turbine using computational analysis and experimental evaluation. The results indicate that flap deployment influenced the lift coefficient, drag coefficient, lift-to-drag ratio, and reported power coefficient under the investigated operating conditions.

The principal findings are summarized as follows:

1. Trailing-edge flap deployment increased the reported lift coefficient across the investigated tip-speed-ratio range. At a tip-speed ratio of 2.5, the lift coefficient increased from 2.34 without flaps to approximately 2.873 with flaps, corresponding to an increase of approximately 22.8%.
2. At a flap deflection angle of 5°, the maximum reported lift coefficient occurred at an angle of attack of 19.5°. The lift coefficient increased from 2.34 without flaps to approximately 2.873 with flaps.

3. Flap deployment also increased the drag coefficient, indicating that the enhancement in lift was accompanied by an aerodynamic drag penalty. Nevertheless, the reported lift-to-drag ratios were higher for the flapped configuration throughout the investigated rotational-speed range.

4. The study reported increases in lift and drag forces of approximately 7.1 N and 3 N, respectively, for the multi-section blade configuration with flaps. However, the corresponding force measurements and operating conditions require verification to establish these differences.

5. The reported turbine starting wind speed decreased from approximately 3 m/s without flaps to 1.4 m/s with flaps, suggesting that flap deployment may improve low-wind-speed starting characteristics. Additional repeated measurements are required to confirm this improvement.

6. The reported improvements in power coefficient were 2.5%, 3.7%, and 4.6% at flap deflection angles of 5°, 10°, and 20°, respectively. The highest reported improvement was associated with a flap angle of 20° and a rotational speed of 343 rpm. However, the calculation method for these percentage improvements requires clarification.

Overall, the findings suggest that trailing-edge flaps have the potential to improve the aerodynamic performance and low-wind-speed operating characteristics of multi-section horizontal-axis wind turbines. However, the observed benefits must be evaluated alongside the additional aerodynamic drag and differences in operating conditions. Further investigations involving matched rotational speeds, independent experimental repetitions, direct torque and power measurements, and aerodynamic flow characterization are recommended to establish the reproducibility and practical significance of the reported improvements.

References

[1] Muheisen, Amer H., Muhammad A. R. Yass, and Ihsan K. Irthiea. “Enhancement of Horizontal Wind Turbine Blade Performance Using Multiple Airfoils Sections and Fences.” Journal of King Saud University – Engineering Sciences 35, no. 1 (2023): 69–81.

[2] Hussein, Hussein Ali, Muhammad A. R. Yass, and Mahmood Abdulzahra Shkara. “Power Optimization of Wind Mill Turbine Blade for Different Cross Section.” Journal of University of Babylon for Engineering Sciences 26, no. 2 (2018): 106–126.

[3] Rasheed, Raghad Majeed, Muhammad A. R. Yass, and Amer Hamad Muhiesen. “Contribution of Lift-to-Drag Ratio on Power Coefficient of HAWT Blade for Different Cross-Sections.” Open Engineering 12, no. 1 (2022): 716–728.

[4] Yass, Muhammad A. R., Ekbal Hussein Ali, and Hussein Ali Hussein. “Experimental Study to Design and Manufacturing of NACA 0012 Horizontal Axis Wind Turbine Blade.” Journal of University of Babylon for Engineering Sciences 26, no. 6 (2018): 128–139.

[5] Xi, Lei, and Lihua Zhao. “Optimal Design of Wind Turbine Blades by Combination of Multi-Airfoil Leaf Elements.” Journal of Physics: Conference Series 2235, no. 1 (2022). IOP Publishing.

[6] Akbari, Vahid, et al. “Multi-Objective Optimization of a Small Horizontal-Axis Wind Turbine Blade for Generating the Maximum Startup Torque at Low Wind Speeds.” Machines 10, no. 9 (2022): 785.

[7] Chaudhary, M. K., and A. Roy. “Design and Optimization of a Small Wind Turbine Blade for Operation at Low Wind Speed.” World Journal of Engineering 12, no. 1 (2015): 83–94.

[8] Schubel, P. J., and R. J. Crossley. “Wind Turbine Blade Design.” Energies 5, no. 9 (2012): 3425–3449.

[9] Blackwood, Marisa. “Maximum Efficiency of a Wind Turbine.” Undergraduate Journal of Mathematical Modeling 6, no. 2 (2016): Article 2.

[10] Mamadaminov, U. M. “Review of Airfoil Structures for Wind Turbine Blades.” Department of Electrical Engineering and Renewable Energy, REE 515 (2013): 1–8.

[11] Kohli, N. K., and E. Ahuja. “HAWT Power Enhancement Using ITS Characteristics.” International Journal of Latest Technology in Engineering, Management & Applied Science 3, no. 1 (2014): 1–7.

[12] Nicolai, Leland M., and Grant E. Carichner. Fundamentals of Aircraft and Airship Design. Volume I: Aircraft Design. American Institute of Aeronautics and Astronautics, 2010.

[13] Younkin, George W. Industrial Servo Control Systems: Fundamentals and Applications, Revised and Expanded. CRC Press, 2002.

[14] Zhang, Dahai, et al. “Unsteady Effects of a Winglet on the Performance of Horizontal-Axis Tidal Turbine.” Renewable Energy 225 (2024): 120334.
[15] Rahnamay Bahambary, Khashayar, et al. “A Numerical Study of Bio-Inspired Wingtip Modifications of Modern Wind Turbines.” Energy (2024): 130561.
[16] Gall, Mihnea, Ion Mălăel, and Dragos Preda. “Computational Analysis of Fence-Type Vertical Axis Wind Turbines Array Suitable for Urban Architecture Integration.” In 2022 26th International Conference on Circuits, Systems, Communications and Computers (CSCC). IEEE, 2022.
[17] Akbari, Vahid, et al. “Multi-Objective Optimization of a Small Horizontal-Axis Wind Turbine Blade for Generating the Maximum Startup Torque at Low Wind Speeds.” Machines 10, no. 9 (2022): 785.
[18] Mohammadi, Mohammadreza, Alireza Mohammadi, and Said Farahat. “A New Method for Horizontal Axis Wind Turbine (HAWT) Blade Optimization.” International Journal of Renewable Energy Development 5, no. 1 (2016): 1–8.
[19] Gertz, D., D. A. Johnson, and N. Swytink-Binnema. “An Evaluation Testbed for Wind Turbine Blade Tip Designs—Winglet Results.” Wind Engineering 36, no. 4 (2012): 389–410.